EVS26
Los Angeles, California, May 6 - 9, 2012

Optimal Dynamic Predictive Cruise Control for differential driven electric vehicles

Joris Janssenswillen[1], Raf Swinnen[2], Sietze Wolfs[3], Peter Slaets[4]
[1]*Joris Janssenswillen (corresponding author)*
Student at Group T- International University College Leuven, joris.janssenswillen@gmail.com
[2]*Raf Swinnen (corresponding author)*
Student at Group T -International University College Leuven, rafswinnen120@hotmail.com
[4]*Sietze Swolfs (corresponding author)*
Research assistent at Group T - International University College Leuven, sietze.swolfs@groept.be
[4]*Peter Slaets (corresponding author)*
Professor at Group T - International University College Leuven, peter.slaets@groept.be

Abstract

This paper describes a method to predict the energy consumption of dual driven electric vehicles (EVs) over a predefined trajectory. This way the voltages that need to be applied on the motors are calculated to optimize the trip for minimal energy consumption and traveling time. Since traveling time and energy consumption are conflicting constraints, the goal is to decrease energy consumption, without entailing a drastic increase in traveling time.
An algorithm was designed to get a weighted optimization for these two constraints, taking into account the trajectory and the aerodynamics of the vehicle. For the aerodynamics also wind velocity and direction are taken into account, combined with the heading of the car. Concerning the trajectory, the route to follow is inserted as a constraint, and the slopes along this route and its environment are taken into account. Using this algorithm, control signals, which are the voltages applied on left and right motor of the vehicle, can be obtained, which make it possible to control the vehicle throughout the trajectory.
The simulation shows that an increase in traveling time has a relatively bigger impact on energy consumption. If direction and wind velocity can be predicted, the algorithm can anticipate on a change in wind velocity, or wind direction. This way the vehicle will consume less energy. Lastly when the trajectory is free to choose by the algorithm, steep slopes will be avoided dependent on the defined weight factor.

Keywords: efficiency, EV(electric vehicles), energy consumption, optimization, range, vehicle performance

1 Introduction

Today, electric drivetrains have become increasingly popular in the automotive industry. Electric drivetrains are characterized by a high power efficiency rate but limited driving range (100-300 km) compared to a regular car (800-1000 km). Extension of the driving range of dual driven EVs powered by brushed DC-motors is the primary goal of this research. To this end a Sequential Quadratic Programming Algorithm is implemented in ACADO [1] to optimize a weighted sum of the energy consumption and travel time along a predefined trajectory. The algorithm takes the effect of trajectory slopes and wind velocity into account. Creating the possibility to

divert slightly from the route, choosing smoother paths and taking the inner bends while cornering. The result of the optimization is a set of motor control voltages for the two DC-motors that control the speed and heading of the vehicle.
Previous research focused on the design of a predictive cruise control for hybrid trucks [2, 3] or the specification of time optimal robot trajectories [4]. In these papers analytical solutions that exploit the opportunities of kinetic energy recovery are derived for the velocity trajectory optimization problem. Combining this technique with the trajectory and aerodynamics based algorithm will result in an energy efficient vehicle, suitable for daily traffic situations.

2 SIMULATION

2.1 Vehicle design

The predictive cruise control described in this paper is solely for dual driven electric vehicles, powered by two brushed DC-motors. The left and right motor power a left and right wheel respectively, by means of two separate gearboxes, with the same gear ratio n. The wheels have a radius r, with inertia J_w. These wheels are positioned on a distance b from the center of the vehicle, with b half of the width as shown in figure 1.

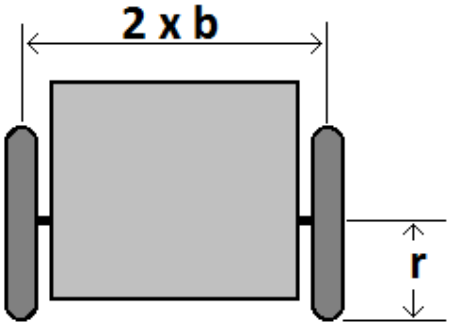

Figure 1: The design of the vehicle.

The inertia of the vehicle for rotation in the horizontal plane about its center of mass is J_c. The angular position of the right and left wheel respectively are given by θ_R and θ_L. The vehicle has mass m. The relationship between right and left wheel angular velocity ω_R, ω_L and vehicle linear and rotational velocity v, ω is:

$$\begin{aligned} v_L &= r \cdot \omega_L, \\ v_R &= r \cdot \omega_R, \\ \omega &= \frac{v_R - v_L}{2b}, \\ v &= \frac{v_R + v_L}{2} \end{aligned} \tag{1}$$

These relationships are shown in figure 2. The nonlinear Cartesian kinematic equations in v, ω and θ then become:

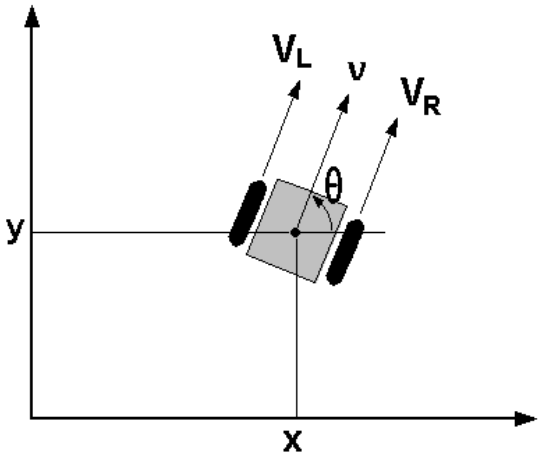

Figure 2: The non-linear relationships of the vehicle.

$$\begin{bmatrix} \dot{x} \\ \dot{y} \\ \dot{\theta} \end{bmatrix} = \begin{bmatrix} v\cos\theta \\ v\sin\theta \\ \omega \end{bmatrix} \tag{2}$$

2.2 Motor model

As stated before, the motors used in this paper consist of brushed DC-motors. Following equations represent the motor dynamics:

$$\mathbf{V} = L\frac{d\mathbf{I}}{dt} + K_{emf}\begin{bmatrix} \omega_R \\ \omega_L \end{bmatrix} + R\mathbf{I} \tag{3}$$

$$\mathbf{T} = K_t\mathbf{I} - c\begin{bmatrix} \omega_R \\ \omega_L \end{bmatrix} + \mathbf{T_L} \tag{4}$$

L, R and $\mathbf{I}$[1] are symbol of inductance, armature resistance and current respectively. K_{emf} and K_t are equal and are torque constant and back emf constant. T_L represents the load torque, described later on in 2.4. The friction in the motor, proportional to the angular velocity is represented by the proportionality constant c. The friction torque is further explained in section 2.4.1. The inductance in the circuit is ignored throughout this paper, because the time constant, to which it leads, in the electric circuit is only small, compared to the mechanical time constant of the system.

2.3 Lagrange model

The total kinetic energy of the vehicle contains the kinetic rotational energy of both wheels around their axle, the vehicle around its center of

[1] All symbols in bold represent vectors.

mass in the horizontal plane and the kinetic translational energy of the total vehicle. The potential energy of the system consists mainly of the elevation, but since an approximation of slopes is used in this model, explained in 2.4.3, this potential energy will not be included in the Lagrangian mechanics [5]. The Lagrangian Ł and the driving forces along the coordinates $F_{\mathbf{q}}$ are given by:

$$\text{Ł}(\mathbf{q}, \dot{\mathbf{q}}) = KE - PE$$
$$F_{\mathbf{q}} = \frac{d}{dt}\left(\frac{\partial \text{Ł}}{\partial \dot{\mathbf{q}}}\right) - \frac{\partial \text{Ł}}{\partial \mathbf{q}} \qquad (5)$$

Thus the Lagrangian becomes:

$$\text{Ł}(\mathbf{q}, \dot{\mathbf{q}}) = \frac{1}{2}m(\dot{x}^2 + \dot{y}^2) + \frac{1}{2}J_c\dot{\theta}^2 + \frac{1}{2}J_w(\omega_R^2 + \omega_L^2)$$

where

$$\mathbf{q} = \begin{bmatrix} \theta_R \\ \theta_L \end{bmatrix}$$

Using relationship (1) to transform all equations to ω_R and ω_L, a dynamic model is obtained after applying equation (5):

$$\text{Ł} = \begin{bmatrix} 1 & 1 \end{bmatrix} \cdot \mathbf{M} \begin{bmatrix} \frac{\omega_R^2}{2} \\ \frac{\omega_L^2}{2} \end{bmatrix}$$
$$\mathbf{M} = \begin{bmatrix} m_{11} & m_{12} \\ m_{21} & m_{22} \end{bmatrix}$$

With

$$m_{11} = m_{22} = \frac{r^2 m}{4} + J_w + \frac{r^2 J_c}{4b^2}$$
$$m_{12} = m_{21} = \frac{r^2 m}{4} - \frac{r^2 J_c}{4b^2}$$

Now the impulses p_{ω_R} and p_{ω_L} and the torques $\mathbf{T}$ become respectively:

$$\begin{bmatrix} p_{\omega_R} \\ p_{\omega_L} \end{bmatrix} = \begin{bmatrix} \frac{\partial L(\mathbf{q},\dot{\mathbf{q}})}{\partial \omega_R} \\ \frac{\partial L(\mathbf{q},\dot{\mathbf{q}})}{\partial \omega_L} \end{bmatrix} = \mathbf{M} \begin{bmatrix} \omega_R \\ \omega_L \end{bmatrix}$$
$$\mathbf{T} = \begin{bmatrix} \frac{dp_{\omega_R}}{dt} \\ \frac{dp_{\omega_L}}{dt} \end{bmatrix} = \mathbf{M}\ddot{\mathbf{q}} \qquad (6)$$

2.4 Load Torque

The load torque consist of three parts: rolling friction, air resistance and the gravitational effect of the slopes, all three are defined as a force acting on the vehicle:

$$T_L = -(F_{drag} + F_{rg} + F_r) \cdot r - T_{fric}$$

This load torque is divided equally over both wheels of the vehicle.

2.4.1 Rolling friction

The rolling friction is proportional to the angular velocity off the vehicle. There is also a friction torque inside the motors, which is proportional to the angular velocity of the motors, this is already taken into account with the constant c in (4). The motors are subjected to a constant friction torque, T_{fric}, which is given in the data sheets.

2.4.2 Air resistance

The second type of resistance this model implies, is the aerodynamic drag force. This force is proportional to the frontal area A_f, the density of the air ρ_a and the square of the speed of the air, relative to the vehicle v_{rel}. The orientation of the car is given by θ. Therefore the orientation of the absolute velocity of the air is defined in the same way, with an angle ϕ. The relative velocity of the air with respect to the car is now given by:

$$v_{rel} = v_{car} - v_{air} \cdot \cos(\phi - \theta)$$

Now the definition of the frontal drag force becomes:

$$F_{drag} = \frac{C_d \cdot A_f \cdot \rho_a \cdot v_{rel}^2}{2}$$

2.4.3 Slope

Normally the effect of slopes is included in the Lagrangian dynamics by means of the potential energy of the system. Here, however, an approximation for the derivatives of the actual elevations with respect to x and y is made.
Interpolation between these slope gives an accurate result for the slope along a certain heading θ. The force due to this slope is now given by:

$$F_{rg} = m \cdot g \cdot sin(\theta_h) \qquad (7)$$

With θ_h the road grade, angle of the slope, in radians. The derivatives of the elevation with respect to x and y are the tangent of the road grade in the x and y direction respectively. With:

$$\nabla h(x,y)_{\overrightarrow{u}} = \frac{\partial h(x,y)}{dx}\cos(\theta) + \frac{\partial h(x,y)}{dy}\sin(\theta)$$

Here $\nabla h(x,y)_{\overrightarrow{u}}$ represents the derivative of $h(x,y)$ in the direction of $\overrightarrow{u}$, equation (7) becomes:

$$F_{rg} = \quad m \cdot g \cdot (sin(\theta_x) \cdot cos(\theta) + sin(\theta_y) \cdot sin(\theta))$$

Figures 3, 4 and 5 show a small hill and its approximations for the slopes in x and y direction respectively.

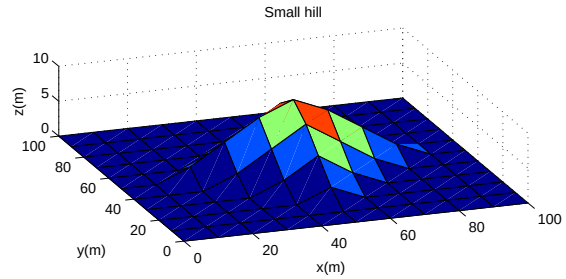

Figure 3: The hill of which an approximation is used in ACADO, it peaks at x,y coordinates (50,50) and has a overall radius of 50 meters.

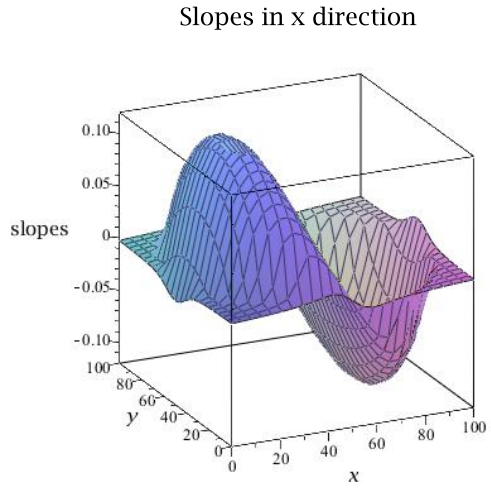

Figure 4: The polynomial approximation of the slopes of the hill in figure 3 in the x-direction.

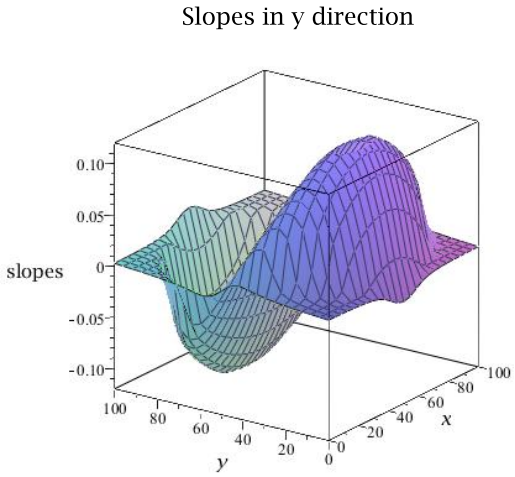

Figure 5: The polynomial approximation of the slopes of the hill in figure 3 in the y-direction.

2.5 State Space Model

After combining the driving torques for the vehicle model, obtained by Lagrange (6) and the motor model equations (3),(4) and solving these equations for $\ddot{\theta}_R$ and $\ddot{\theta}_L$, a state space model can be obtained:

$$\dot{\mathbf{q}} = \mathbf{A_{mot}}\mathbf{q} + \mathbf{B_{mot}}\mathbf{U}$$

$$\mathbf{U} = \begin{bmatrix} V_R \\ V_L \\ T_R \\ T_L \end{bmatrix}$$

$$\mathbf{A_{mot}} = \begin{bmatrix} a_{11} & a_{12} \\ a_{21} & a_{22} \end{bmatrix}$$

$$\mathbf{B_{mot}} = \begin{bmatrix} b_{11} & b_{12} \\ b_{21} & b_{22} \end{bmatrix} \begin{bmatrix} 1 & 0 & \frac{R}{K_t} & 0 \\ 0 & 1 & 0 & \frac{R}{K_t} \end{bmatrix}$$

With:

$$a_{11} = -\frac{(c\,R + K_t\,K_{emf})\left(b^2 r^2 m + 4\,J_w\,b^2 + r^2 J_c\right)}{R\,(2\,J_w\,b^2 + r^2 J_c)\,(r^2 m + 2\,J_w)}$$

$$a_{11} = a_{22}$$

$$a_{12} = a_{21} = \frac{(c\,R + K_t\,K_{emf})\,r^2\left(b^2 m - J_c\right)}{R\,(2\,J_w\,b^2 + r^2 J_c)\,(r^2 m + 2\,J_w)}$$

$$b_{11} = b_{22} = \frac{K_t\left(b^2 r^2 m + 4\,J_w\,b^2 + r^2 J_c\right)}{R\,(2\,J_w\,b^2 + r^2 J_c)\,(r^2 m + 2\,J_w)}$$

$$b_{12} = b_{21} = -\frac{K_t\,r^2\left(b^2 m - J_c\right)}{R\,(2\,J_w\,b^2 + r^2 J_c)\,(r^2 m + 2\,J_w)}$$

Where $\mathbf{q} = [\omega_R, \omega_L]^T$. Using equations (1), this model can be transformed to v and ω, the velocity and angular velocity of the vehicle respectively using $\mathbf{P}$:

$$\mathbf{P} = \begin{bmatrix} \frac{r}{2} & \frac{r}{2} \\ \frac{-r}{2 \cdot b} & \frac{r}{2 \cdot b} \end{bmatrix}$$

$$\begin{bmatrix} v \\ \omega \end{bmatrix} = \mathbf{P} \begin{bmatrix} \omega_R \\ \omega_L \end{bmatrix}$$

This means that the matrices $\mathbf{A_{mot}}$ and $\mathbf{B_{mot}}$ change to:

$$\mathbf{A} = \mathbf{P}\mathbf{A_{mot}}\mathbf{P^{-1}} = \begin{bmatrix} a_{11} & 0 \\ 0 & a_{22} \end{bmatrix}$$

$$\mathbf{B} = \mathbf{P}\mathbf{B_{mot}} = \begin{bmatrix} b_{11} & b_{12} & b_{13} & b_{14} \\ b_{21} & b_{22} & b_{23} & b_{24} \end{bmatrix}$$

With:

$$a_{11} = -2\,\frac{c\,R + K_t\,K_{emf}}{(r^2 m + 2\,J_w)\,R}$$
$$a_{22} = -2\,\frac{(c\,R + K_t\,K_{emf})\,b^2}{(2\,J_w\,b^2 + r^2 J)\,R}$$
$$b_{11} = b_{12} = \frac{r\,K_t}{(r^2 m + 2\,J_w)\,R}$$
$$b_{13} = b_{14} = \frac{r}{(r^2 m + 2\,J_w)}$$
$$b_{21} = b_{22} = \frac{b\,r\,Kt}{(2\,J_w\,b^2 + r^2 J)\,R}$$
$$b_{23} = b_{24} = \frac{b\,r}{(2\,J_w\,b^2 + r^2 J)}$$

The state space model now becomes:

$$\dot{\mathbf{X}} = \mathbf{A}\mathbf{X} + \mathbf{B}\mathbf{U}$$

With:

$$\mathbf{X} = \begin{bmatrix} v \\ \omega \end{bmatrix}$$

This state space model is a system of first order differential equations in v and ω with inputs V_R, V_L, T_R and T_L[2], the applied voltages on the right and left motor and the known disturbance torques on the right and left wheel respectively. This model can be used in ACADO to optimize for a weighted minimum in travel time and consumed energy.

2.6 Constraints

The model described in the previous section is subjected to several constraints.

2.6.1 Motor

The first set of constraints is necessary and follows from the choice of motor. Each motor is restricted to a certain working area, defined by limits of angular velocity, current, voltage and power. T_e denotes the total traveling time. The constraints of the motor must always be obeyed.

Angular velocity This is the limit on the rotational speed of the motors, for the sake of the bearings.

$$\forall t \in [0, T_e]:$$
$$-\omega_{max} \leq \omega_R(t) \leq \omega_{max}$$
$$-\omega_{max} \leq \omega_L(t) \leq \omega_{max}$$

[2]Note that the load torques on both wheels are not actually inputs to the system, but disturbances. Their value can be predicted and used in the optimization.

Current Current is limited between a negative and a positive value. Both are the same size in absolute value. The negative sign means that energy is recuperated or the car is driving backwards. The values can be found in the data sheet of the motor.

$$\forall t \in [0, T_e]:$$
$$-I_{max} \leq I_R(t) \leq I_{max}$$
$$-I_{max} \leq I_L(t) \leq I_{max}$$

Voltage The voltage can vary between zero and a maximum positive value, which is also derived from the data sheet, in absolute value.

$$\forall t \in [0, T_e]:$$
$$-U_{max} \leq U_R(t) \leq U_{max}$$
$$-U_{max} \leq U_L(t) \leq U_{max}$$

Power Limit on power delivered by the motors or applied to the motors when they are in generator operation.

$$\forall t \in [0, T_e]:$$
$$-P_{max} \leq P_R(t) \leq P_{max}$$
$$-P_{max} \leq P_L(t) \leq P_{max}$$

2.6.2 Track

The second set of constraints is based on the predefined trajectory and initial and final conditions. These conditions are necessary for longer routes, where the route has to be divided in smaller sections, for the sake of accuracy. Each section has its own approximations for x and y slopes and the trajectory to follow.

Initial conditions At the start, the vehicle has a velocity of 0 m/s. The vehicle will accelerate to a certain speed at the end of the subsection of the route. When the calculation of control signals of the previous section is finished, the next section will start with the same speed in which the previous ended. The same applies to the starting angle θ and Cartesian coordinates x and y.

$$x(0) = [v(0), x(0), y(0), \omega(0), \theta(0)]^T$$

Final conditions The vehicle needs final conditions, a final position with a heading, a transversal and rotational velocity.

$$x(T_e) = [v(T_e), x(T_e), y(T_e), \omega(T_e), \theta(T_e)]^T$$

Path The vehicle has to stay between an upper and lower boundary which resemble the sides of the road. These boundaries make it possible to take inner bends, which is better for both time and energy consumption. The road boundaries are approximated by polynomial functions in function of the Cartesian coordinates of the car, x and y, such that these functions can be inserted in a constraint in ACADO.

$$0 \geq f_{outer}(x, y)$$
$$0 \leq f_{inner}(x, y)$$

Bend velocity The torque delivered by the motors on the wheels is limited by the friction available between the wheels and the ground. Also, while cornering, the speed is limited, because of the danger to slip or tilt. The vehicle is assumed to slip before it will tilt, therefore only the first case is applied as a constraint. The car will slip when the total interaction force between a wheel and the ground exceeds the maximum friction force. This total interaction force consists of two parts. The first part is a longitudinal part, in the direction of the wheel, caused by the traction of the car, the delivered torque by the motor. The second part is a transversal force, normal to the direction of the wheel, which is caused by lane keeping, centrifugal forces while taking bends.

$$F_{total} = \sqrt{F_{centrifugal}^2 + F_{traction}^2} \leq F_{friction}$$
$$F_{friction} = N \cdot \mu$$
$$F_{centrifugal} = r \cdot \omega^2$$

With N the normal force acting between wheel and road and r the radius of the wheel:

$$r = \frac{v}{\omega}$$
$$F_{traction} = \frac{T_{wheel}}{r}$$

So the constraint becomes:

$$\left(\frac{T_{wheel}}{r}\right)^2 + (v \cdot \omega)^2 \leq (N \cdot \mu)^2$$

2.7 Cost Function

For the optimization for both consumed energy and travel time, a cost function must be defined, with both variables. This combination is done by means of a weight parameter w, which stands for the importance of consumed energy in the optimization:

$$C(x(t), u(t)) = w * (E_R + E_L) + (1 - w) * T$$

Here E_R and E_L are the consumed energy of the right and left motor respectively and T is the total travel time. It is of great importance to define the parameter w in function of several other parameters, such that the reasonable results are obtained in all situations, whether it is about an electric kart or an electric truck. The truck will consume much more energy and thus using the same weight parameter for both vehicles would lead to a much longer travel time for the truck. It is obvious that the mass of the vehicle plays an important role in the definition of the weight parameter, but the frontal area for example also has a significant effect on the consumed energy by means of the aerodynamic drag force. Not only parameters of the vehicle are important, a hilly landscape will lead to more consumed energy than a flat landscape, therefore the weight parameter is dependent on the trajectory as well. It is very difficult to define this weight parameter, because time and consumed energy are two total different quantities. The energy is often a lot bigger than the traveling time. Therefore the weight parameter would be very small. The relative increase in energy is the same as the relative increase in time for this cost function. When this percentage of energy increase is small, the time increase with the same percentage will be even smaller.

3 RESULTS

Table 1: Electric Kart Parameters.

Motor Parameters		
I_{max}	200 A	Maximum current
ω_{max}	534 rad/s	Maximum angular velocity
V_{max}	80 V	Maximum voltage
P_{max}	16000 W	Maximum power
R_a	0.032 Ω	Armature resistance
K_t	0.14 Nm/A	Torque constant
K_{emf}	0.14 vs/rad	Back emf constant
Vehicle Parameters		
b	0.6 m	Half width
h	0.85 m	Height
m	240 kg	Mass
C_d	0.3	Aerodynamic drag coefficient
l	1.7 m	Length
n	3	Gear ratio
c	8.432e-3	Angular friction coefficient
μ	0.9	Friction between wheel and ground
J_w	0,02 kgm^2	Moment of inertia of wheels
m_w	2.16 kg	Mass of wheel
r	0.14 m	Radius of wheel

To test the effectiveness of the algorithm, a simulation has been done on a virtual surface. he surface consisted of an area of 100 by 100 meters, containing a small hill in the center. This surface is differentiated in both the x and y direction. Polynomial approximations of these slopes were then used in the algorithm as the definition of the environment in which the vehicle was driving. As vehicle, an electric kart is used. The parameters of the kart are shown in table 1.
A set of different situations is applied on the algorithm to explore several types of benefits the algorithm can produce.

3.1 Inner bends

First of all, the simplest case of all, a situation has been applied to inspect whether the vehicle takes inner bends while cornering. It is easy to see that this would be the optimal solution for both the minimal consumed energy optimization and the minimal traveling time optimization. The situation applied consists of several constraints:

1. Begin position and orientation:
   $x = 0\,m; y = 0\,m; \theta = 0\,radians$
2. Final position:
   $y = 100\,m$
3. Inner path constraint:
   $90^2 \leq (y - 100)^2 + x^2$
4. Outer path constraint:
   $110^2 \geq (y - 100)^2 + x^2$

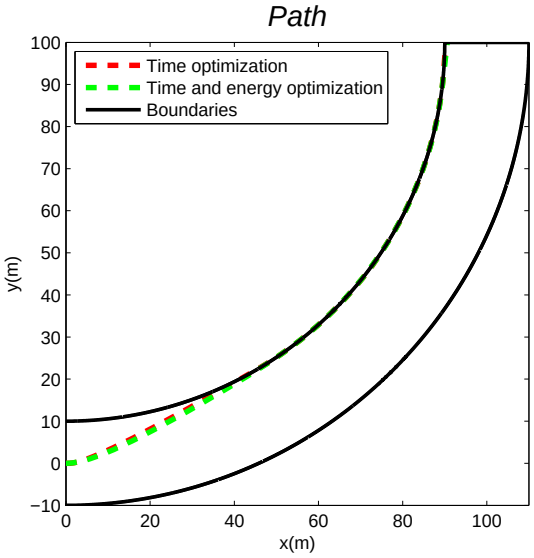

Figure 6: The paths of the vehicle in the xy-plane are visualized by means of dashed lines. The solid lines represent the borders of the road.

The vehicle is thus restricted to the area between the two circles, it starts at the origin with an orientation to the east[3], the vehicle has to reach $y = 100$. The algorithm will search for the optimal path to get there. It is easily seen that the weight parameter has little influence, since energy and time are both minimal when taking the inner bend, the weight will only have an effect on the velocity of the vehicle. In figure 6 the solution of the algorithm is shown. When optimizing with respect to energy as well, the vehicle turns slower towards the inner boundary.

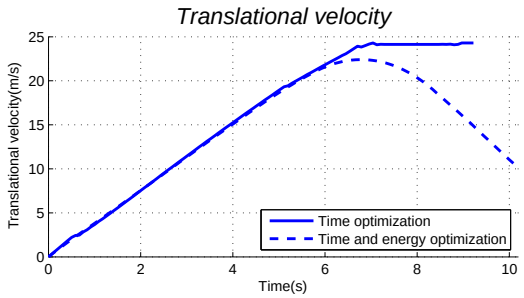

Figure 7: The velocity of the vehicle in function of the traveled time.

Figure 7 shows the velocity of the vehicle when the weight parameter emphasizes the traveling time and both traveling time and energy to be optimal. Compared with the optimization for time only, it is noticed that the vehicle decelerates as it approaches the goal, when the weight emphasizes both energy and time. The vehicle reaches its maximum velocity[4] while optimizing solely to time.

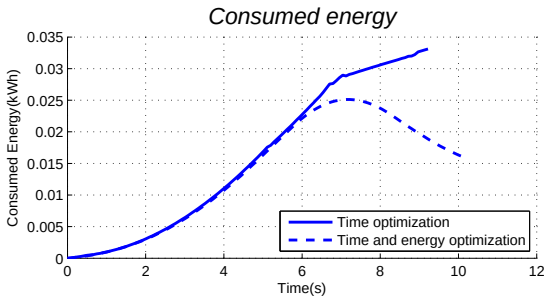

Figure 8: The consumed energy of the vehicle.

Figure 8 shows the consumed energy in time with the time optimization and the combination of time and energy. An increase of 10.4% in time is the cost for the consumed energy to drop with 52.0%, with the used weight. Note that this energy drop and time increase has nothing to do with the taking of inner bends, because both weights lead to the taking of the inner bend. The deceleration at the end, caused by the combination weight, causes the time to increase and the energy to drop, because energy is recuperated while braking. Note however that the time based

[3] Directed to the positive x-axis.
[4] The maximum velocity followed by constraint 2.6.1

optimization is the worst case scenario considering consumed energy, as can be seen in figure 7, the vehicle is at every instant accelerating, until it reaches its maximum velocity.

3.2 Aerodynamic drag

In this second case two wind directions are applied in the same trajectory. The wind changes suddenly to the opposite direction when x becomes greater than 75 meters. This sudden wind change is a virtual situation, to inspect whether the optimization anticipates such changes. For instance when the vehicle is subjected to a strong tail wind, but must make a U-turn in the near future, changing this tail wind into a strong head wind. The trajectory is free to choose by the algorithm, the final position, however, is $x = 150m$, so the vehicle will experience a tail wind in the first half and a head wind in the second:

1. Begin position and orientation:
   $x = 0m; y = 0m; \theta = 0radians$

2. Final position:
   $x = 150m$

The wind has in both cases a velocity of 10 m/s, which is equivalent to 5 Beaufort, a strong wind. The results of the optimizations are shown in figures 9 and 10, the path turned out to be a straight line, which is logical since this wind can not be avoided.

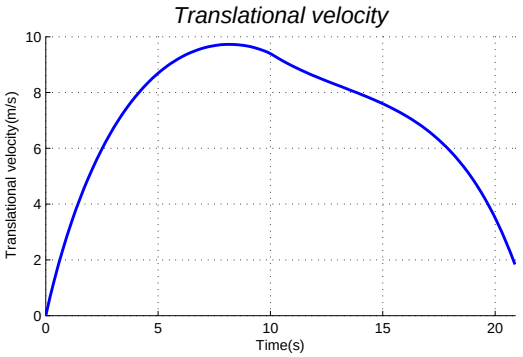

Figure 9: The velocity of the vehicle in function of traveled time, with a tail wind in the first 12 seconds and a head wind after 12 seconds.

As can be seen in figure 9, the vehicle decelerates when approaching the sudden wind change. Since a kart is used in the simulation, the aerodynamic drag force is relatively small. Therefore the change in velocity the vehicle makes, to anticipate the change in wind, is relatively small. The drag force is proportional to the second order of the velocity, so a small decrease in velocity to a bigger decrease in drag force. This considerably smaller drag force consumes a lot less energy.

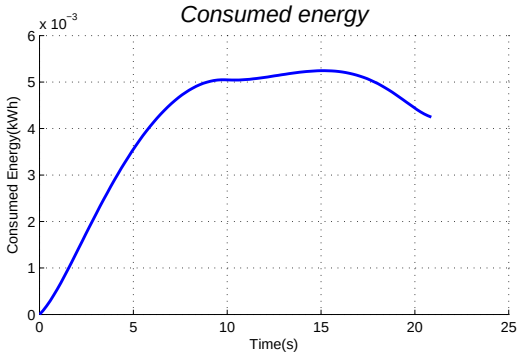

Figure 10: The consumed energy of the vehicle in function of traveled time, with a tail wind in the first 12 seconds and a head wind after 12 seconds.

3.3 Slopes

It is interesting to explore the effect of slopes on the optimization. Therefore the vehicle is placed near a small hill, as shown in 3. This hill is a virtual surface, designed especially for this test. The vehicle has initial position $(0, 40)$ in meters and has to reach the final position $(100, 40)$, while the hill peaks at $(50, 50)$. The slopes in both x and y direction are shown in figures 4 and 5 respectively. The algorithm has been executed several times, each time slightly emphasizing the consumed energy more in the optimization. As expected, the vehicle avoids steep slopes more and more when optimizing more towards minimal energy. The evolution of the path of the vehicle can be seen in figure 12. The evolution in consumed energy is shown in figure (11).

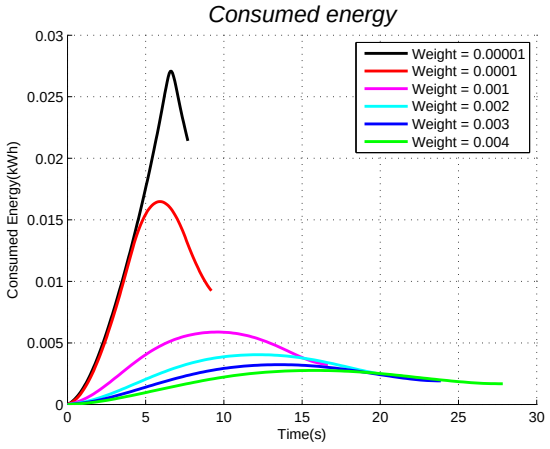

Figure 11: The evolution of the consumed energy of the vehicle in function of time, when optimizing more and more towards minimal energy.

The evolution of the endpoints in this figure form a pareto front[6]. The change in energy between the optimizations with weight 0.00001 and 0.0001 is big considering the change in traveling time it causes. Upward of weight 0.001, the increase in time is much to large considering the

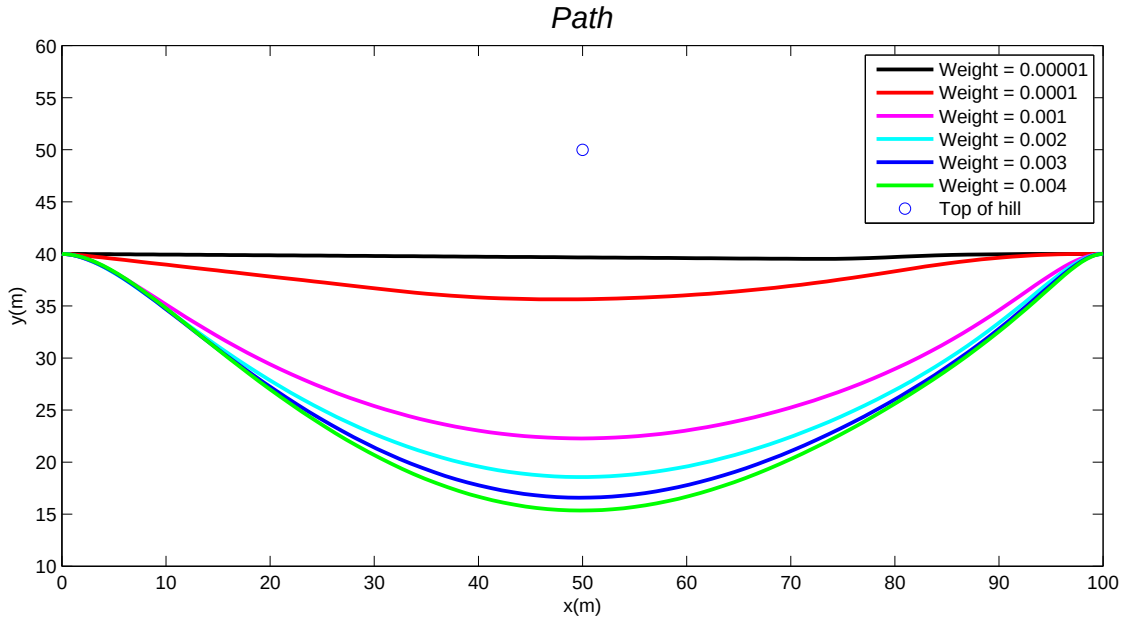

Figure 12: The evolution of the path of the vehicle, when optimizing more and more towards minimal energy. The top of the hill is indicated by the small circle at (50,50), the hill has a radius of 50 meters.

drop in energy it causes.

4 DISCUSSION

During the development of the algorithm several problems were encountered. Most of the problems were eventually solved.

4.1 Accuracy

First of all, the accuracy of the approximations is still low. By using the derivatives of the route directly, instead of using the altitudes, the accuracy is improved. However, The coordinates that are used are not perfect, they have a deviation of more or less two meters. These accuracies are amplified by approximating the tracks and surfaces to mathematical formulas. This lack of accuracy could be solved by using a look-up table and a closed loop controller to limit the inaccuracies. The inaccuracies of the GPS-signal will be dramatically improved with the introduction of the new Galileo satellites in the near future [7]. The use of look-up tables instead of approximations for the data at hand would make the algorithm a lot more accurate.

4.2 Calculation time

Secondly, the calculation needs to be done off line, because computing the optimal control signals is time consuming. An on line calculation would be much more interesting. This problem could be solved by using look-up tables as well. At this moment the algorithm has to calculate several complex formulas at each calculation, it is clear that a look-up table requires a lot less computation time.

4.3 Weight formula

The weight parameters used in these simulations are estimates, determined by trial and error. This factor is function of several parameters, as mentioned before, like mass and aerodynamics of the vehicle, relief of the route, etc. By defining a formula for this factor, the cost function can be calculated by a computer, so no human intervention is needed.

4.4 Efficiencies

The efficiency of the transmission is considered perfect, while a more realistic value should be more or less 95%. This assumption has little effect on the results of the simulation discussed in this paper. The model must resemble reality as good as possible. It would be interesting to include an efficiency map[5] of the motors in the optimization, this can be done as future work, in form of a look-up table.

4.5 Discontinuities

Several formulas needed in the model of the vehicle included discontinuities, for the differential states in ACADO however, there is no such thing

[5] An efficiency map displays the efficiencies of the motors in function of angular velocity and torque delivered by the motor.

as a sign or a step function. It was possible to obtain a sign function by use of the absolute value of a state:

$$sign(x) = \frac{x}{\sqrt{x^2}}$$

But the calculation of powers requires more calculation time. Therefore another solution is used, namely the use of sigmoid functions. These are continuous functions which resemble step or sign functions. In this model a sigmoid function based on the arctangent is used:

$$sign(x) \simeq \frac{2 \cdot \arctan(10,000 \cdot x)}{\pi} \qquad (8)$$

The factor $10,000$ is used to make better approximation of the discontinuous sign function. Equation (8) is shown in figure 13.

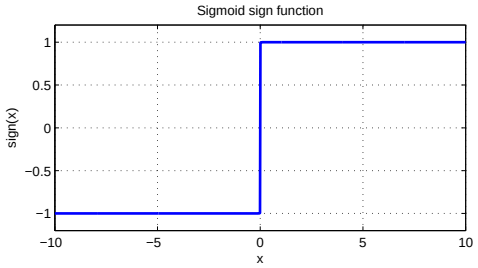

Figure 13: The approximation of the sign function with use of the sigmoid function arctangent.

There are two cases in which this sigmoid function needs to be used: air resistance and constant friction torque.

Air resistance The aerodynamic drag force acting on the vehicle is of second order in the relative speed of the air to the vehicle. A second order function, however, is never negative, while the sign of this force should change sign at the point where the relative velocity of the air to the car becomes zero. This is because the force changes direction at this point.

$$F_{drag} = \frac{C_d \cdot A_f \cdot \rho_a \cdot v_{rel}^2}{2} \cdot \frac{2 \cdot \arctan(10,000 \cdot v_{rel})}{\pi}$$

Constant friction The vehicle is subjected to a constant friction torque, this friction torque, however, changes sign at velocity zero. Therefore the sigmoid function is used in this case as well. When velocities are positive, a constant torque acts on the wheels in the negative direction, when velocities are negative, a constant torque acts on the wheels in the positive direction, at standstill no friction torque is applied:

$$T_{fric} = T_0 \cdot \frac{2 \cdot \arctan(10,000 \cdot v)}{\pi}$$

5 SUMMARY AND CONCLUSIONS

This paper is a first step towards optimization of driving style to obtain an extended driving range for future electric vehicles. The main advantage is that no drastic changes need to be done in battery packs or drive trains. However, the model is limited because no real life traffic situations are taken into account, such as traffic jam, speed limits, slipstreams, etc. Further investigation in optimizing the follow up distance between vehicles [8] and consideration of the instantaneous energy consumption needs to be done, to make the algorithm suitable for daily traffic situations. Also constraints on maximum speed need to be implemented to resemble speed limits. Secondly the weight parameter needs to be optimized. It would be interesting to use a formula instead of the weight, with parameters dependent on mass, aerodynamics of the vehicle and relief of the trajectory. By improving calculation time, the algorithm can be used for on line calculation. This way it can be integrated in a commercial GPS-system, where trajectories are calculated by using start point and destination. A simplified algorithm of this model can be used for efficient train transportation, since diverting from the route can be disregarded and only one motor needs to be controlled. Future research can be done to extend this model so it can be used for driving agricultural vehicles through a hilly landscape.

References

[1] B. Houska, H. Ferreau, and M. Diehl, "ACADO Toolkit – An Open Source Framework for Automatic Control and Dynamic Optimization," *Optimal Control Applications and Methods*, vol. 32, no. 3, pp. 298–312, 2011.

[2] T. van Keulen, G. Naus, B. de Jager, R. van de Molengraft, M. Steinbuch, and E. Aneke, "Predictive cruise control in hybrid electric vehicles," *World Electric Vehicle Journal*, vol. 3, May 2009.

[3] T. van Keulen, B. de Jager, A. Serrarens, and M. Steinbuch, "Optimal energy management in hybrid electric trucks using route information," *Oil & Gas Science and Technology*, vol. 65, no. 1, pp. 103–113, 2010.

[4] D. Verscheure, M. Diehl, J. D. Schutter, and J. Swevers, "On-line time-optimal path tracking for robots," in *ICRA*, 2009, pp. 599–605.

[5] D. A. Wells, *Lagrangian Dynamics*, ser. Schaum's Outlines. McGraw-Hill, Inc., 1967.

[6] J. S. and Arora, "Chapter 17 - multi-objective optimum design concepts

and methods," in *Introduction to Optimum Design (Third Edition)*, third edition ed. Boston: Academic Press, 2012, pp. 657–679. [Online]. Available: http://www.sciencedirect.com/science/article/pii/B9780123813756000176

[7] ESA, "Galileo in tune: first navigation signal transmitted to earth," Dec. 2011. [Online]. Available: http://www.test.org/doe/http://www.esa.int/esaNA/SEMIC88XZVG_index_0.html

[8] G. Naus, R. van den Bleek, J. Ploeg, B. Scheepers, M. van de Molengraft, and M. Steinbuch, "Explicit mpc design and performance evaluation of an acc stop-&-go," in *American Control Conference, 2008*, 2008, pp. 224–229.